

SHOCK BREAKOUT DRIVEN BY THE REMNANT OF A NEUTRON STAR BINARY MERGER: AN X-RAY PRECURSOR OF MERGERNOVA EMISSION

SHAO-ZE LI AND YUN-WEI YU

Draft version April 23, 2018

ABSTRACT

A supra-massive neutron star (NS) spinning extremely rapidly could survive from a merger of NS-NS binary. The spin-down of this remnant NS that is highly magnetized would power the isotropic merger ejecta to produce a bright mergernova emission in ultraviolet/optical bands. Before the mergernova, the early interaction between the NS wind and the ejecta can drive a forward shock propagating outwards into the ejecta. As a result, a remarkable amount of heat can be accumulated behind the shock front and the final escaping of this heat can produce a shock breakout emission. We describe the dynamics and thermal emission of this shock with a semi-analytical model. It is found that sharp and luminous breakout emission appears mainly in soft X-rays with a luminosity of $\sim 10^{45}$ erg s⁻¹ at a few hours after the merger, by leading the mergernova emission as a precursor. Therefore, detection of such an X-ray precursor would provide a smoking-gun evidence for identifying NS-powered mergernovae and distinguishing them from the radioactive-powered ones (i.e., kilonovae or macronovae). The discovery of NS-powered mergernovae would finally help to confirm the gravitational wave signals due to the mergers and the existence of supra-massive NSs.

Subject headings: gamma-ray burst: general — stars: neutron — supernovae: general

1. INTRODUCTION

A merger of binary neutron stars (NSs) is one of the most promising targets of direct detection of gravitational waves (GWs). Such a detection pointing to a few hundred Mpc is expected to come true in the very near future with the second generation of ground-based GW detectors (Abadie et al. 2010; Nissanke et al. 2013). For achieving such an expectation, some observations of electromagnetic counterparts of the GW signals are necessarily needed, which can help to confirm the position, time, redshift, and astrophysical properties of the GW sources.

During a NS-NS merger event, the rapidly rotating compact system could eject a highly collimated relativistic jet and a quasi-isotropic sub-relativistic outflow, where various electromagnetic emission could be produced. Specifically, internal and external dissipations of the jet energy can result in a short-duration gamma-ray burst (GRB) and its multi-wavelength afterglow emission, which could be the most attractive electromagnetic counterparts in view of their high brightness (see Nakar 2007, Berger 2014 for reviews). However, unfortunately, the detection probability of an associated GRB is significantly suppressed by the small opening angle of the jet (Fong et al. 2014), although a late and weak orphan afterglow could still be observed by off-axis (van Eerten & MacFadyen 2011; Metzger & Berger 2012). Alternatively, more and more attentions have been paid to the emission originating from the isotropic ejecta, e.g., thermal emission due to the diffusion of internal energy of the ejecta (called mergernova by Yu et al. 2013; Li & Paczynski 1998; Kulkarni 2005; Rosswog 2005; Metzger et al. 2010) and non-thermal emission due to the shock interaction between the ejecta and environment medium

(Nakar & Piran 2011; Metzger & Berger 2012; Piran et al. 2013; Gao et al. 2013).

The isotropic merger ejecta is probably highly neutron-rich, which makes it possible to effectively synthesize nuclei much heavier than ⁵⁶Ni via rapid neutron capture processes (r-processes; Rosswog et al. 1999, 2014; Roberts et al. 2011; Goriely et al. 2011; Korobkin et al. 2012; Bauswein et al. 2013a; Hotokezaka et al. 2013, 2015; Wanajo et al. 2014; Goriely 2015; Just et al. 2015; Martin et al. 2015). The radioactive decays of these newly synthesized elements can heat the ejecta to produce a detectable thermal emission. However, being limited by the low mass of the ejecta (no more than a few percent of solar mass) and the element synthesis efficiency, the luminosity of a radioactive-powered mergernova is expected to be not much higher than $\sim 10^{41}$ erg s⁻¹. Thus these phenomena are widely known as kolinova or macronova (Kulkarni 2005; Metzger et al. 2010; Barnes & Kasen 2013; Tanaka & Hotokezaka 2013; Grossman et al. 2014; Kasen et al. 2015a).

Such a luminosity limit can be breached if a more powerful energy source can be provided by the central post-merger compact object. By invoking a remnant supra-massive NS that spins extremely rapidly and is highly magnetized, Yu et al. (2013) and Metzger & Piro (2014) investigated the characteristics of mergernova emission with an energy injection from the spin-down of the NS. It was found that the peak luminosity of such a NS-powered mergernova, which of course depends on the lifetime of the NS and the collimation of the NS wind, could sometimes be comparable to and even exceed the luminosity of ordinary supernovae, but with a much shorter duration on the order of a few days. Excitingly, some unusual rapidly evolving and luminous transients were discovered by some recent observations such as the Pan-STARRS1 Medium Deep Survey (Drout et al. 2014). The characteristics of these transients are

¹ Institute of Astrophysics, Central China Normal University, Wuhan 430079, China, yuyw@mail.ccnu.edu.cn

basically consistent with the predictions for NS-powered mergernovae (Yu et al. 2015), although multi-wavelength cross-identifications are still demanded.

Recently some multi-wavelength studies have already been carried out on observational candidates of mergernovae. For example, being indicated by the shallow-decay afterglows of GRB 130603B, the widely-discussed infrared excess after this GRB is argued to be probably powered by a remnant NS (Fan et al. 2013) rather than by radioactivities as usually considered (Tanvir et al. 2013; Berger et al. 2013). More directly, by considering of the high-energy emission from a NS wind (Yu et al. 2010; Zhang 2013), which can partly leak from a preceding merger ejecta at late time, a NS-powered mergernova is expected to be possibly accompanied by a late X-ray re-brightening. Very recently Gao et al. (2015) found that the late optical and X-ray bumps after GRB 080503 provided a perfect sample for such multi-wavelength features. In this paper, going ahead, we would reveal another possible X-ray signature prior to a NS-powered mergernova, which is caused by the breakout of the shock arising from the early interaction between the NS wind and the merger ejecta. This X-ray precursor emission would play an essential role in future mergernova identifications and in GW detections.

2. THE MODEL

2.1. Remnant neutron star and merger ejecta

A merger would happen inevitably in a NS-NS binary when the gravity between the NSs can no longer be supported by angular momentum because of GW radiation release. After the merger, in some situations, a supra-massive NS rather than a black hole could be left with an extremely rapid differential rotation. This is supported indirectly by many emission features of short GRBs and afterglows including extended gamma-ray emission, X-ray flares, and plateaus (Dai et al. 2006; Fan & Xu 2006; Zhang 2013; Giacomazzo & Perna 2013; Rowlinson et al. 2010, 2013). The presence of such a supra-massive NS is permitted by both theoretical simulations (Bauswein et al. 2013b; Hotokezaka et al. 2011) and observational constraints (e.g., the present lower limit of the maximum mass of Galactic NSs is precisely set by PSR J0348+0432 to $2.01 \pm 0.04 M_\odot$; Antoniadis et al. 2013). During the first few seconds after the birth of a remnant NS, on one hand, a great amount of neutrinos can be emitted from the very hot NS. On the other hand, differential rotation of the NS can generate multipolar magnetic fields through some dynamo mechanisms (Duncan & Thompson 1992; Price & Rosswog 2006; Cheng & Yu 2014), making the NS to be a magnetar. Consequently, during the very early stage, the neutrino emission and ultra-strong magnetic fields together could drive a continuous baryon outflow (Dessart et al. 2009; Siegel et al. 2014; Siegel & Ciolfi 2015), which provides an important contribution to form an isotropic merger ejecta. A few of seconds later, the NS eventually enters into an uniform rotation stage and meanwhile a stable dipole structure of magnetic fields can form. From then on, the NS starts to lose its rotational energy via a Poynting flux-dominated wind. The spin-down luminosity carried by the wind can be estimated with the magnetic dipole radiation formula as $L_{\text{sd}} = L_{\text{sd},i} (1 + t/t_{\text{md}})^{-2}$, where $L_{\text{sd},i} =$

$10^{47} \mathcal{R}_{s,6}^6 \mathcal{B}_{14}^2 \mathcal{P}_{i,-3}^{-4} \text{ erg s}^{-1}$, $t_{\text{md}} = 2 \times 10^5 \mathcal{R}_{s,6}^{-6} \mathcal{B}_{14}^{-2} \mathcal{P}_{i,-3}^2 \text{ s}$, and the zero point of time t is set at the beginning of the magnetic dipole radiation which is somewhat later than the NS formation by several seconds. Here \mathcal{R}_s , \mathcal{B} , and \mathcal{P}_i are the radius, dipolar magnetic field strength, and initial spin periods of the NS, respectively, and the convention $Q_x = Q/10^x$ is adopted in cgs units.

During a merger event, although the overwhelmingly majority of matter falls finally into the central remnant NS, there is still a small fraction of matter ejected outwards, e.g., the baryon wind blown from the NS mentioned above. Besides that component, a quasi-isotropic merger ejecta can also be contributed by a wind from a short-lived disk surrounding the NS, by an outflow from the colliding interface between the two progenitor NSs, and by a tidal tail due to the gravitational and hydrodynamical interactions. The latter two components are usually called dynamical components. These ejecta components differ with each other in masses, electron fractions, and entropies. It is difficult and nearly impossible to describe precisely the specific constituents and distributions of a merger ejecta, which depend on the relative sizes of the two progenitor NSs, equation of states of NS matter, and magnetic field structures. In any case, according to the numerical simulations in literature, on one hand, the mass of dynamical components could range from $\sim 10^{-4} M_\odot$ to a few times $\sim 0.01 M_\odot$ (Oechslin et al. 2007; Bauswein et al. 2013a; Hotokezaka et al. 2013; Rosswog 2013). On the other hand, in presence of a remnant supra-massive NS, the mass of a neutrino-driven wind is found to be at least higher than $3.5 \times 10^{-3} M_\odot$ (Perego et al. 2014), and the mass-loss rate due to ultra-high magnetic fields is about $10^{-3} - 10^{-2} M_\odot \text{ s}^{-1}$ during the first 1 – 10 s (Siegel et al. 2014). Therefore, by combining all of these contributions (see Rosswog 2015 for a brief review), we would take $M_{\text{ej}} = 0.01 M_\odot$ as a reference value for the total mass of an ejecta. Furthermore, we would adopt power-law density and velocity distributions of this mass as follows (Nagakura et al. 2014):

$$\rho_{\text{ej}}(r, t) = \frac{(\delta - 3) M_{\text{ej}}}{4\pi r_{\text{max}}^3} \left[\left(\frac{r_{\text{min}}}{r_{\text{max}}} \right)^{3-\delta} - 1 \right]^{-1} \left(\frac{r}{r_{\text{max}}} \right)^{-\delta} \quad (1)$$

and

$$v_{\text{ej}}(r, t) = v_{\text{max}} \frac{r}{r_{\text{max}}(t)}, \quad \text{for } r \leq r_{\text{max}}(t), \quad (2)$$

where r is the radius to the central NS, v_{max} is the maximum velocity of the head of ejecta which is probably on the order of $\sim 0.1c$, and the slope δ ranges from 3 to 4 according to the numerical simulation of Hotokezaka et al. (2013). We fix $\delta = 3.5$ as in Nagakura et al. (2014). The variation of δ within a wide range in fact cannot significantly affect the primary results of this paper except for an extremely high value (e.g. $\delta > 5$). The maximum radius of ejecta can be calculated by $r_{\text{max}}(t) \approx r_{\text{max},i} + v_{\text{max}} t$, where $r_{\text{max},i} \approx v_{\text{max}} \Delta t$ with Δt being the time on which the dipolar magnetic field is stabilized. Correspondingly, the minimum radius reads $r_{\text{min}}(t) = r_{\text{min},i} + v_{\text{min}} t$ and its initial value could be determined by an escape radius as $r_{\text{min},i} = (2GM_c r_{\text{max},i}^2 / v_{\text{max}}^2)^{1/3}$, where G is the gravitational constant and M_c is the mass of the remnant NS.

The huge energy released from a remnant NS (i.e. millisecond magnetar) would eventually drive an ultra-relativistic wind mixing Poynting flux and leptonic plasma, which catches up with the preceding merger ejecta very quickly. On one hand, if this wind always keeps Poynting-flux-dominated even until it collides with the ejecta, the material at the bottom of ejecta could be heated by absorbing low-frequency electromagnetic waves from the Poynting component. On the other hand, more probably, some internal dissipations (e.g. the IC-MART processes; Zhang & Yan 2011) could take place in the NS wind to produce non-thermal high-energy emission. Subsequently, a termination shock could be formed at the interface between the wind and ejecta, if the wind magnetization has become sufficiently low there (Mao et al. 2010). As a result, the bottom of ejecta can be heated by absorbing high-energy photons from the emitting wind region and/or by transmitting heat from the neighbor hot termination-shock region. Additionally, even if we arbitrarily assume an extreme situation that all of the wind energy is completely reflected from the interface, the bottom material of ejecta would also be heated due to adiabatic compression by the high pressure of the wind. Therefore, in any case, the energy carried by the wind can always be mostly injected into the bottom of ejecta and heat the material there.

2.2. Shock heating and emission

When the bottom of a merger ejecta is heated by an injected NS wind, a pressure balance can be built naturally between the wind and the ejecta bottom. On one hand, the pressure balance can gradually extend to larger radii through thermal diffusion, which however happens very slowly for an extremely optical thick ejecta. On the other hand, the high pressure of the bottom material can lead itself to expand adiabatically and to get a high speed. This speed would result in the formation of a forward shock propagating outwards into the ejecta.

By denoting the radius and speed of a shock front by r_{sh} and v_{sh} , respectively, the increase rate of the mass of shocked ejecta can be calculated by

$$\frac{dM}{dt} = 4\pi r_{\text{sh}}^2 [v_{\text{sh}} - v_{\text{ej}}(r_{\text{sh}}, t)] \rho_{\text{ej}}(r_{\text{sh}}, t), \quad (3)$$

where $v_{\text{ej}}(r_{\text{sh}}, t)$ and $\rho_{\text{ej}}(r_{\text{sh}}, t)$ are the velocity and density of the upstream material just in front of the shock. Obviously, we also have $dr_{\text{sh}} = v_{\text{sh}} dt$. As the propagation of the shock, its bulk kinetic energy, which is previously gained from adiabatic acceleration, can again be partly converted into internal energy of the newly shocked material. The rate of this shock heating effect can be written as

$$H_{\text{sh}} = \frac{1}{2} [v_{\text{sh}} - v_{\text{ej}}(r_{\text{sh}}, t)]^2 \frac{dM}{dt}. \quad (4)$$

Then the total internal energy accumulated by the shock, U_{sh} , can be derived from

$$\frac{dU_{\text{sh}}}{dt} = H_{\text{sh}} - P_{\text{sh}} \frac{d(\epsilon V)}{dt} - L_{\text{sh}}. \quad (5)$$

Here $P_{\text{sh}} = U_{\text{sh}}/(3\epsilon V)$ is an average pressure, $V \sim (4/3)\pi r_{\text{sh}}^3$ is the volume of the whole shocked region experiencing an adiabatic expansion, and the fraction ϵ is

introduced by considering that the shock-accumulated heat is mostly deposited at a small volume immediately behind the shock front. The product of this average pressure and the corresponding volume represents the cooling effect due to adiabatic expansion. L_{sh} is the luminosity of shock thermal emission, which is caused by the diffusion and escaping of the shock heat.

Approximately following a steady diffusion equation $L = (4\pi r^2/3\kappa\rho)(\partial u/\partial r)c$, where κ is opacity, ρ and u are densities of mass and internal energy, respectively, we roughly estimate the luminosity of shock thermal emission by

$$L_{\text{sh}} \approx \frac{r_{\text{max}}^2 U_{\text{sh}} c}{\epsilon r_{\text{sh}}^3 + (r_{\text{max}}^3 - r_{\text{sh}}^3)} \left[\frac{1 - e^{-(\epsilon\tau_{\text{sh}} + \tau_{\text{un}})}}{\epsilon\tau_{\text{sh}} + \tau_{\text{un}}} \right], \quad (6)$$

where $\tau_{\text{sh}} = \kappa M/4\pi r_{\text{sh}}^2$ and $\tau_{\text{un}} = \int_{r_{\text{sh}}}^{r_{\text{max}}} \kappa \rho_{\text{ej}} dr$ are the optical depths of the shocked and unshocked ejecta, respectively. Here the former optical depth, which only influences the decrease of the shock emission after breakout, is calculated by considering that the most of shocked material is concentrated within a thin shell behind the shock front (Kasen et al. 2015b). The value of parameter ϵ can be fixed by equating the shock luminosity during breakout to the simultaneous heating rate, because after that moment freshly-injected shock heat can escape from the ejecta nearly freely. The opacity of merger ejecta is predicted to be on the order of magnitude of $\sim (10 - 100) \text{ cm}^2 \text{ g}^{-1}$, which results from the bound-bound, bound-free, and free-free transitions of lanthanides synthesized in the ejecta (Kasen et al. 2013). This value is much higher than the typical one of $\kappa = 0.2 \text{ cm}^2 \text{ g}^{-1}$ for normal supernova ejecta. In this paper we take $\kappa = 10 \text{ cm}^2 \text{ g}^{-1}$. Fairly speaking, some reducing effects on the opacity could exist, e.g., (1) the lanthanide synthesis in the wind components of ejecta could be blocked by neutrino irradiation from the remnant NS by enhancing electron fractions (Metzger & Fernández 2014) and (2) the lanthanides in the dynamical components could be ionized by the X-ray emission from the NS wind (Metzger & Piro 2014).

2.3. Shock dynamics

The temporal evolution of shock thermal emission, as presented in Equation (6), is obviously dependent on the dynamical evolution of the shock. Due to the slow thermal transmission in the optical thick ejecta, a significant pressure/temperature gradient must exist in the ejecta during shock propagation, which would lead the shock to be continuously accelerated. Therefore, the dynamical evolution of such a radiation-mediated shock is completely different from the internal and external shocks in GRB situations. For an optical thin GRB ejecta, a pressure balance can be built throughout the whole shocked region simultaneously with the shock propagation. In that case, the shock velocity can be simply derived from shock jump conditions (Dai 2004; Yu & Dai 2007; Mao et al. 2010). On the contrary, in the present optical thick case, a detailed dynamical calculation of the shock in principle requires an elaborate description of the energy and mass distributions of the ejecta (see Kasen et al. 2015b for a 1D hydrodynamical simulation for a similar process), which is however beyond the scope of an analytical model. Nevertheless, a simplified and effective

dynamical equation can still be obtained by according to the energy conservation of the system.

The total energy of the shocked region, can be written as $E = \frac{1}{2} M v_{\text{sh}}^2 + U$, where U is the total internal energy of the shocked region. For a radiation-mediated shock, the value of U should be much higher than U_{sh} . In principle, the concept “shocked region” used here can generally include the NS wind regions, because the mass of wind leptons is drastically smaller than that of shocked ejecta and, more importantly, the energy released from the NS is continuously distributed in both the wind and ejecta through thermal diffusion, which makes them behaving like a whole. By ignoring the relatively weak energy supply by radioactivities, the variation of the total energy can be written as

$$dE = (\xi L_{\text{sd}} - L_e) dt + \frac{1}{2} v_{\text{ej}}^2(r_{\text{sh}}, t) dM, \quad (7)$$

where ξ represents the energy injection efficiency from the NS wind, which could be much smaller than one if the NS wind is highly anisotropic, and L_e is the total luminosity of the thermal emission of merger ejecta. As a general expression, the specific form of the energy injection is not taken into account. Substituting the expression of E into Equation (7), we can get the dynamical equation of the forward shock as

$$\frac{dv_{\text{sh}}}{dt} = \frac{1}{M v_{\text{sh}}} \left[(\xi L_{\text{sd}} - L_e) - \frac{1}{2} (v_{\text{sh}}^2 - v_{\text{ej}}^2) \frac{dM}{dt} - \frac{dU}{dt} \right] \quad (8)$$

In order to clarify the expressions of L_e and dU/dt , we denote $\tilde{U} = U - U_{\text{sh}}$, which represents the internal energy excluding the shock-accumulated part. The evolution of this internal energy component can be given by

$$\frac{d\tilde{U}}{dt} = \xi L_{\text{sd}} - \tilde{P} \frac{dV}{dt} - L_{\text{mn}}, \quad (9)$$

where the adiabatic cooling is also calculated with an average pressure as $\tilde{P} = \tilde{U}/3V$ and

$$L_{\text{mn}} \approx \frac{\tilde{U} c}{r_{\text{max}}} \left[\frac{1 - e^{-(\tau_{\text{sh}} + \tau_{\text{un}})}}{\tau_{\text{sh}} + \tau_{\text{un}}} \right]. \quad (10)$$

The above expression is different from Equation (6) because the majority of internal energy of the shocked region is deposited in the most inner part of the region, which is much deeper than the shock front. Then we have $L_e = L_{\text{sh}} + L_{\text{mn}}$. The emission component represented by L_{mn} actually is the mergernova emission discussed in Yu et al. (2013).

By substituting Equations (4), (5), and (9) into (8), we can obtain another form of the dynamical equation as

$$\frac{dv_{\text{sh}}}{dt} = \frac{1}{M v_{\text{sh}}} \left(\frac{U}{3V} \right) \frac{dV}{dt}, \quad (11)$$

which is just the expression adopted in Kasen et al. (2015b) to calculate the shock breakout for super-luminous supernovae. This equation can be easily understood in the framework of adiabatic acceleration of a “fireball”. As discussed above, what accelerating the

² For simplicity, in this paper we do not taken into account the relativistic effects that were considered in Yu et al. (2013) for some extremely light ejecta.

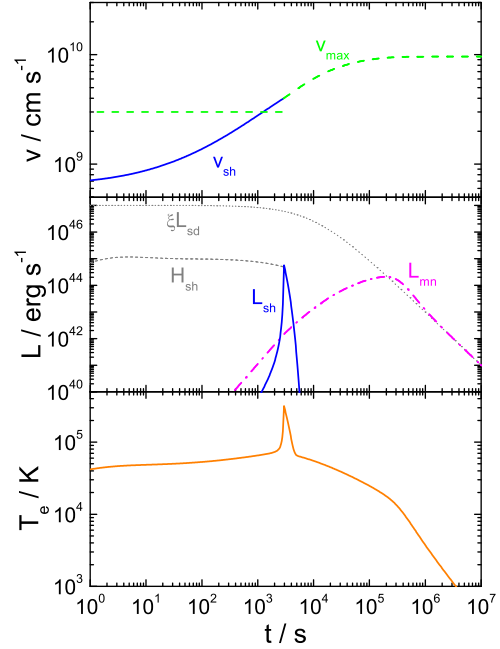


FIG. 1.— Evolutions of velocities (top), bolometric luminosities (middle), and emission temperature (bottom). In the middle panel, the injected spin-down luminosity (ξL_{sd}) and the shock heating rate (H_{sh}) are also presented for references. The model parameters are taken as $\xi L_{\text{sd},i} = 10^{47} \text{ erg s}^{-1}$, $t_{\text{md}} = 10^4 \text{ s}$, $\Delta t = 2 \text{ s}$, $M_{\text{ej}} = 0.01 M_{\odot}$, $v_{\text{max}} = 0.1c$, $\delta = 3.5$, and $\kappa = 10 \text{ cm}^2 \text{ g}^{-1}$.

ejecta material is actually the local internal pressures at different radii, which are much lower than the pressure of the NS wind due to the significant delay of pressure transmission. The work done by these varying pressures can be effectively estimated with an average internal pressure of $(U/3V)$ with respect to a volume variation of $dV = 4\pi r_{\text{sh}}^2 v_{\text{sh}} dt$. With the above dynamical equation, the energy conservation and assignments of the system can be well described. By considering that the internal energy at the time t is on the order of magnitude $U \sim L_{\text{sd}} t$, Equation (11) can naturally determine a kinetic energy also on the same order of magnitude $\frac{1}{2} M v_{\text{sh}}^2 \sim L_{\text{sd}} t$.

3. RESULTS AND ANALYSES

A supra-massive NS surviving from a merger event is believed to initially spin with a Keplerian limit period of about 1 ms. This corresponds to a rotational energy of several times 10^{52} erg with a high stellar mass, which could be much higher in view of the rapid differential rotation. The most of this energy is probably consumed very quickly to generate and amplify magnetic fields, to drive a short GRB, and maybe also to radiate GWs. The duration of this violent stage should not be much longer than the duration of the short GRB. So we would take $\Delta t = 2 \text{ s}$ which is the boundary dividing long and short GRBs. When a steady magnetic dipole radiation begins, the spin period could have been reduced to a few milliseconds, corresponding to an energy of $\sim 10^{51-52} \text{ erg}$. This energy supply could be further discounted for the merger ejecta by the parameter ξ , if a remarkable fraction is collimated within a small cone to power an extended gamma-ray emission and X-ray afterglow plateau after

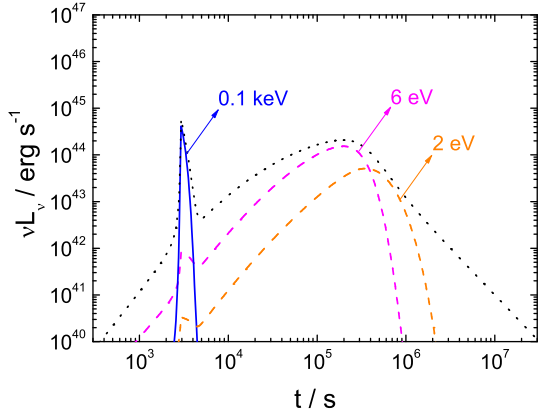


FIG. 2.— Three chromatic light curves for photon energies of $h\nu = 0.1$ keV (soft X-ray; solid), 6 eV (UV; dashed), and 2 eV (optical; dash-dotted), respectively, where the bolometric light curve (dotted) is presented for a reference.

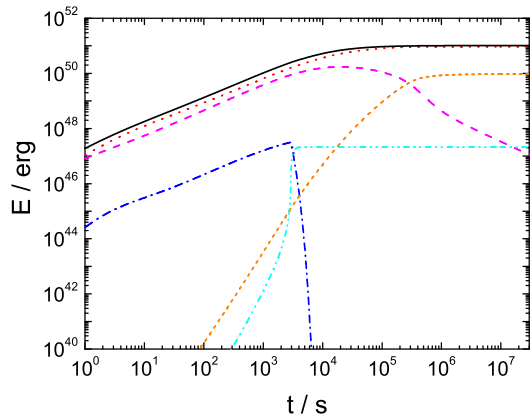


FIG. 3.— Cumulations of different energy components. Solid black line: total energy provided by the NS; Dotted red line: kinetic energy of shocked ejecta; Dashed magenta line: internal energy \tilde{U} ; Dash-dotted blue line: shock-produced internal energy U_{sh} ; Dash-dot-dotted cyan line: energy of shock emission; Short-dashed orange line: energy of mergernova emission.

the GRB.

For typical values of spin-down luminosity and timescale as $\xi L_{\text{sd},i} = 10^{47} \text{ erg s}^{-1}$ and $t_{\text{md}} = 10^4$ s, we present a representative numerical result in Figure 1. As shown in the top panel, the shock initially moves slowly, with a velocity much smaller than the maximum velocity of ejecta, and experiences a gradual acceleration process. When the shock velocity exceeds the maximum ejecta velocity by about a few tens percentage, shock breakout happens, as indicated by the sharp peak in the middle panel. It takes a remarkably long time ($\sim 10^3$ s) by the shock to break out from the ejecta. This period is much longer than the shock breakout time given in some previous works ($\sim 1 - 10$ s; Gao et al. 2013; Wang et al. 2015; Siegel & Ciolfi 2015a,b), because there the shock velocity was significantly overestimated by using shock jump conditions with an assumed global pressure balance. However, as discussed above, such a global pressure balance actually cannot be built very quickly for a radiation-mediated shock. The internal energy produced

by the shock only occupies a very small fraction of the total internal energy behind the shock. The shock jump conditions could be satisfied only after a very long time acceleration or after the ejecta is close to optical thin, before which the shock has already crossed the whole ejecta. The middle panel of Figure 1 also shows the shock breakout emission is very luminous, which is comparable to that of the following bright mergernova emission peaking at a few days. Nevertheless, since the shock breakout and mergernova are emitted at very different radii, the corresponding emission temperature ($\sim 10^5$ K) of the former can be much higher than the latter ($\sim 10^4$ K), as presented in the bottom panel. Here an effective temperature is defined by $T_e = (L_e/4\pi r_{\text{max}}^2 \sigma)^{1/4}$ with σ being the Stefan-Boltzmann constant. In more details, we further plot three chromatic light curves in Figure 2, by assuming a black-body spectrum³

$$\nu L_\nu = \frac{8\pi^2 r_{\text{max}}^2}{h^3 c^2} \frac{(h\nu)^4}{\exp(h\nu/kT_e) - 1} \quad (12)$$

with temperatures given in the bottom panel of Figure 1, where h is the Planck constant and k the Boltzmann constant. As shown, while the mergernova emission falls into the ultraviolet band, the shock breakout is mainly concentrated within soft X-rays, for the adopted model parameters. Finally, in order to verify some energy arguments mentioned above, we plot the temporal evolutions of different energy components in Figure 3. It is exhibited that, although the energy released from the NS is initially injected into the ejecta in the form of internal energy, the majority of this internal energy is finally converted into the kinetic energy of the ejecta. As a result, during the whole optical thick period, the internal and kinetic energies keep to be basically comparative with each other. The internal energy produced by the shock is obviously less than the injected one but, at the shock breakout time, the instantaneous release of this small amount of energy can still temporarily overshadow the emission component due to the thermal diffusion.

For a straightforward understanding of the characteristics of the shock breakout emission, here we provide some analytical analyses. Firstly, in physics, shock breakout happens when the dynamical time begins to be longer than the diffusion timescale on which photons diffuse from the shock front to the outmost surface of merger ejecta. Hence we can in principle solve the shock breakout time t_{bo} from the equation

$$t_{\text{bo}} = t_d = \left(\frac{r_{\text{max}} - r_{\text{sh,bo}}}{\lambda} \right)^2 \frac{\lambda}{c} = \frac{(r_{\text{max}} - r_{\text{sh,bo}})^2 \kappa \rho_{\text{ej}}}{c}, \quad (13)$$

³ In Yu et al. (2013), this spectrum is incorrectly written with an internal temperature rather than the effective surface temperature used here, although the integrated bolometric luminosity there is still right because of the reduction by optical depth. More strictly, the surface temperature in fact should be defined at a photosphere radius, beyond which photons can escape freely, rather than the maximum radius. Nevertheless, before the mergernova peak emission, the difference between these two radii actually is always negligible (e.g., see Equation 14). Thus we approximately use the maximum radius here for simplicity. The shift of the photosphere in the ejecta could significantly influence the mergernova emission mainly after the peak time (Wang et al. 2015).

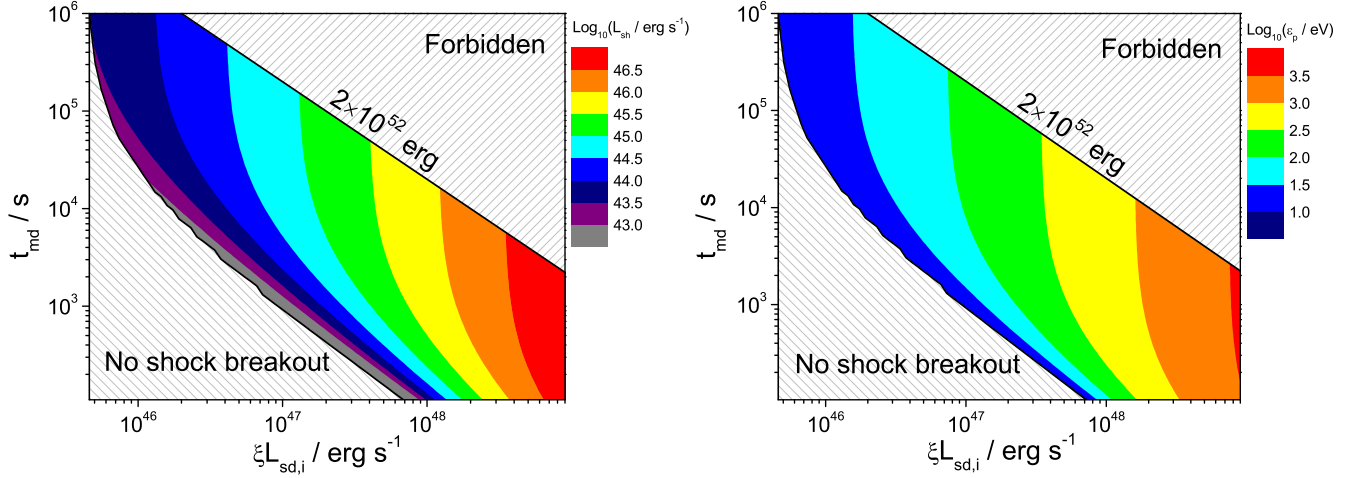


FIG. 4.— Variations of the luminosity (left) and peak photon energy (right) of shock breakout emission in the $\xi L_{\text{sd},i} - t_{\text{md}}$ parameter space. The shaded region on the right-top corner is forbidden because an unrealistically high rotational energy is required, while in the left-bottom shaded region the shock breakout is buried in the mergernova emission.

where $\lambda = 1/(\kappa\rho_{\text{ej}})$ is the average path of photons. Approximately we get

$$r_{\text{sh,bo}} \approx r_{\text{max}} \left(1 - \frac{r_{\text{max}}}{r_*} \right), \quad (14)$$

where $r_* \approx (v_{\text{max}}\kappa M_{\text{ej}}/c)^{1/2} = 4.5 \times 10^{15} \text{ cm}$ ($v_{\text{max}}/0.1c)^{1/2}(\kappa/10 \text{ cm}^2 \text{ g}^{-1})^{1/2}(M_{\text{ej}}/0.01 M_{\odot})^{1/2}$. This means, when the shock breakout happens, the shock radius has been very close to the maximum radius of ejecta. By invoking $U \sim \xi L_{\text{sd}} t$, $P = U/(3V)$, and acceleration rate $a \sim 4\pi r_{\text{sh}}^2 P/M$, we can estimate the breakout radius by $r_{\text{sh,bo}} \sim \frac{1}{2} a t_{\text{bo}}^2 \sim (\xi L_{\text{sd}}/2M_{\text{ej}})^{1/2} t_{\text{bo}}^{3/2}$, where $M \approx M_{\text{ej}}$ is adopted because $r_{\text{sh,bo}} \approx r_{\text{max}}$. Then, from the equation $r_{\text{sh,bo}} \approx r_{\text{max}} = v_{\text{max}} t_{\text{bo}}$, we can simply derive the shock breakout time to

$$t_{\text{bo}} \sim \frac{2M_{\text{ej}} v_{\text{max}}^2}{\xi L_{\text{sd}}} = 3600 \text{ s} \left(\frac{v_{\text{max}}}{0.1c} \right)^2 \left(\frac{M_{\text{ej}}}{0.01 M_{\odot}} \right) \left(\frac{\xi L_{\text{sd}}}{10^{47} \text{ erg s}^{-1}} \right)^{-1} \quad (15)$$

Furthermore we get $v_{\text{sh,bo}} \sim 2v_{\text{max}}$ and $r_{\text{sh,bo}} \sim 2M_{\text{ej}} v_{\text{max}}^3 / \xi L_{\text{sd}} = 1.1 \times 10^{13} \text{ cm}$ that is indeed much smaller than r_* . Then the luminosity and temperature of shock breakout can be estimated to

$$L_{\text{sh,bo}} \approx H_{\text{sh}} \sim 2\pi r_{\text{sh,bo}}^2 (v_{\text{sh,bo}} - v_{\text{max}})^3 \rho_{\text{ej}} \sim 8 \times 10^{45} \text{ erg s}^{-1} \left(\frac{\xi L_{\text{sd}}}{10^{47} \text{ erg s}^{-1}} \right), \quad (16)$$

and

$$T_{\text{sh,bo}} = \left(\frac{L_{\text{sh,bo}}}{4\pi r_{\text{max}}^2 \sigma} \right)^{1/4} \sim 6 \times 10^5 \text{ K} \times \left(\frac{v_{\text{max}}}{0.1c} \right)^{-3/2} \left(\frac{M_{\text{ej}}}{0.01 M_{\odot}} \right)^{-1/2} \left(\frac{\xi L_{\text{sd}}}{10^{47} \text{ erg s}^{-1}} \right)^{3/4} \quad (17)$$

The above analytical expressions qualitatively exhibits the physical mechanisms and the parameter-dependencies of the shock breakout emission, although the numbers given here are somewhat higher than the

numerical ones because a linear acceleration is assumed. It is indicated that the dependence of the shock breakout emission on the density profile of the merger ejecta (i.e., the parameter δ) is very weak. In more details, in Figure 4 we present the variations of the shock breakout luminosity $L_{\text{sh,bo}}$ and the peak photon energy $\varepsilon_p = 4kT_{\text{sh,bo}}$ in the $\xi L_{\text{sd},i} - t_{\text{md}}$ parameter space. It is indicated that, for a significantly bright shock breakout emission, a large amount of energy is required to be released from a NS within a sufficiently short time.

4. CONCLUSION AND DISCUSSIONS

Mergernovae, in particular, the ones powered by a remnant supra-massive NS, are one of the most competitive electromagnetic counterparts of GW signals during NS-NS mergers. The discovery of NS-powered mergernovae could also substantially modify and expand our conventional understandings of supernova-like transient phenomena. Therefore, it would be an usual and essential question that how to identify a mergernova in future searchings and observations. Undoubtedly, a multi-wavelength method is necessary and helpful for answering this question. In this paper, we uncover that a shock breakout can be driven by the early interaction between a merger ejecta and a succeeding NS wind. Such a breakout appears at a few hours after the merger, by leading the mergernova emission as a precursor. The breakout emission would be mainly in soft X-rays with a luminosity of $\sim (10^{44} - 10^{46}) \text{ erg s}^{-1}$, corresponding to an X-ray flux of a few $\times (10^{-11} - 10^{-9}) \text{ erg s}^{-1} \text{ cm}^{-2}$ for a distance of $\sim 200 \text{ Mpc}$, which can be above the sensitivity of many current and future telescopes, e.g., Swift X-ray telescope (Burrows et al. 2005), Einstein Probe (Yuan et al. 2015), etc. More optimistically, some X-ray shock breakout emission could have been appeared in some X-ray afterglows of short GRBs, which probably exhibits as an early X-ray flare. It will be interesting to find out such candidates.

This work is supported by the National Basic Research Program of China (973 Program, grant 2014CB845800), the National Natural Science Foundation of China (grant

No. 11473008), and the Program for New Century Excellent Talents in University (grant No. NCET-13-0822).

REFERENCES

- Abadie, J., Abbott, B. P., Abbott, R., et al. 2010, *CQGra*, 27, 173001
- Antoniadis, J., Freire, P. C. C., Wex, N., et al. 2013, *Science*, 340, 448
- Barnes, J., & Kasen, D. 2013, *ApJ*, 775, 18
- Bauswein, A., Goriely, S., & Janka, H. T. 2013a, *ApJ*, 773, 78
- Bauswein, A., Baumgarte, T. W., & Janka, H. T. 2013b, *Phys. Rev. Lett.*, 111, 131101
- Berger, E., Fong, W., & Chornock, R. 2013, *ApJ*, 774, L23
- Berger, E. 2014, *ARA&A*, 52, 43
- Burrows, D. N., et al. 2005, *Space Sci. Rev.*, 120, 165
- Cheng, Q., & Yu, Y. W. 2014, *ApJ*, 786, L13
- Dai, Z. G. 2004, *ApJ*, 606, 1000
- Dai, Z. G., Wang, X. Y., Wu, X. F., & Zhang, B. 2006, *Science*, 311, 1127
- Dessart, L., Ott, C. D., Burrows, A., et al. 2009, *ApJ*, 690, 1681
- Duncan, R. C., & Thompson, C. 1992, *ApJ*, 392, L9
- Fan, Y. Z., & Xu, D. 2006, *MNRAS*, 372, L19
- Fan, Y. Z., Yu, Y. W., Xu, D., et al. 2013, *ApJ*, 779, L25
- Fong, W., Berger, E., Metzger, B. D., et al. 2014, *ApJ*, 780, 118
- Gao, H., Ding, X., Wu, X. F., et al. 2013, *ApJ*, 771, 86
- Gao, H., Ding, X., Wu, X. F., et al. 2015, *ApJ*, 807, 163
- Giacomazzo, B., & Perna, R. 2013, *ApJ*, 771, L26
- Goriely, S., Bauswein, A., & Janka, H. T. 2011, *ApJ*, 738, L32
- Goriely, S. 2015, *The European Physical Journal A*, 51, 22
- Grossman, D., Korobkin, O., Rosswog, S., & Piran, T. 2014, *MNRAS*, 439, 757
- Hotokezaka, K., Kyutoku, K., Okawa, H., et al. 2011, *Phys. Rev. D*, 83, 124008
- Hotokezaka, K., Kiuchi, K., Kyutoku, K., et al. 2013, *Phys. Rev. D*, 87, 024001
- Hotokezaka, K., & Piran, T. 2015, *MNRAS*, 450, 1430
- Just, O., Bauswein, A., Pulpillo, R. A., et al. 2015, *MNRAS*, 448, 541
- Kasen, D., Badnell, N. R., & Barnes, J. 2013, *ApJ*, 774, 25
- Kasen, D., Fernández, R., & Metzger, B. D. 2015a, *MNRAS*, 450, 1777
- Kasen, D., Metzger, B. D., & Bildsten, L. 2015b, *arXiv:1507.03645v2*
- Korobkin, O., Rosswog, S., Arcones, A., & Winteler, C. 2012, *MNRAS*, 426, 1940
- Kulkarni, S. R. 2005, *arXiv: astro-ph/0510256*
- Li, L. X., & Paczyński, B. 1998, *ApJ*, 507, L59
- Martin, D., Perego, A., Arcones, A., et al. 2015, *arXiv:1506.05048*
- Mao, Z., Yu, Y. W., Dai, Z. G., et al. 2010, *A&A*, 518, 27
- Metzger, B. D., Martinez-Pinedo, G., Darbha, S., et al. 2010, *MNRAS*, 406, 2650
- Metzger, B. D., & Berger, E. 2012, *ApJ*, 746, 48
- Metzger, B. D., & Fernández, R. 2014, *MNRAS*, 441, 3444
- Metzger, B. D., & Piro, A. L. 2014, *MNRAS*, 439, 3916
- Nakar, E. 2007, *PhR*, 442, 166
- Nakar, E., & Piran, T. 2011, *Nature*, 478, 82
- Nagakura, H., Hotokezaka, K., Sekiguchi, Y., et al. 2014, *ApJ*, 784, L28
- Nissanke, S., Holz, D. E., Dalal, N., et al. 2013, *arXiv:1307.2638*
- Oechslin, R., Janka, H. T., & Marek, A. 2007, *A&A*, 467, 395
- Perego, A., Rosswog, S., Cabezón, R. M., et al. 2014, *MNRAS*, 443, 3134
- Piran, T., Nakar, E., & Rosswog, S. 2013, *MNRAS*, 430, 2121
- Price, D. J., & Rosswog, S. 2006, *Science*, 312, 719
- Roberts, L. F., Kasen, D., Lee, W. H., et al. 2011, *ApJ*, 736, L21
- Rosswog, S., Liebendörfer, M., Thielemann, F. K., et al. 1999, *A&A*, 341, 499
- Rosswog, S. 2005, *ApJ*, 634, 1202
- Rosswog, S. 2013, *Royal Society of London Philosophical Transactions Series A*, 371, 20120272
- Rosswog, S., Korobkin, O., Arcones, A., et al. 2014, *MNRAS*, 439, 744
- Rosswog, S. 2015, *IJMPD*, 24, 1530012
- Rowlinson, A., O'Brien, P. T., Tanvir, N. R., et al. 2010, *MNRAS*, 409, 531
- Rowlinson, A., O'Brien, P. T., Metzger, B. D., et al. 2013, *MNRAS*, 430, 1061
- Siegel, D. M., Ciolfi, R., & Rezzolla, L. 2014, *ApJ*, 785, L6
- Siegel, D. M., & Ciolfi, R. 2015, In *Proceedings of Swift: 10 Years of Discovery, PoS(SWIFT 10)169*(Trieste, Italy: Proceedings of Science, SISSA)
- Siegel, D. M., & Ciolfi, R. 2015a, *arXiv: 1508.07911*
- Siegel, D. M., & Ciolfi, R. 2015b, *arXiv: 1508.07939*
- Tanaka, M., & Hotokezaka, K. 2013, *ApJ*, 775, 113
- Tanvir, N. R., Levan, A. J., Fruchter, A. S., et al. 2013, *Nature*, 500, 547
- van Eerten, H. J., & MacFadyen, A. I. 2012, *ApJ*, 747, L30
- Wanajo, S., Sekiguchi, Y., Nishimura, N., et al. 2014, *ApJ*, 789, L39
- Wang, L. J., Dai, Z. G., & Yu, Y. W. 2015, *ApJ*, 800, 79
- Wang, L. J., et al. 2015, *ApJ*, submitted
- Yu, Y. W., & Dai, Z. G. 2007, *A&A*, 470, 119
- Yu, Y. W., Cheng, K. S., & Cao, X. F. 2010, *ApJ*, 715, 477
- Yu, Y. W., Zhang, B., & Gao, H. 2013, *ApJ*, 776, L40
- Yu, Y. W., Li, S. Z., & Dai, Z. G. 2015, *ApJ*, 806, L6
- Yuan, W., Zhang, C., Feng, H. et al., 2015, *arXiv:1506.07735*
- Zhang, B., & Yan, H. R. 2011, *ApJ*, 726, 90
- Zhang, B. 2013, *ApJ*, 763, L22